energies

MDPI

Article

Evaluation of Voltage Variations Arising from the Increase in Photovoltaic Insertion in the Transmission Network: Case Study Coremas-PB Power Plant

Fábio Xavier Lobo [1], Gustavo Fernandes de Negreiros [2], Igor Cavalcante Torres [3] and Chigueru Tiba [2,*]

[1] Department of Electrical Engineering, Federal Institute of Pernambuco (IFPE), Pesqueira 55200-000, Brazil; fabio.lobo@ufpe.br
[2] Department of Nuclear Energy, Federal University of Pernambuco (UFPE), Recife 50670-901, Brazil
[3] Center for Agrarian Sciences (CECA), Federal University of Alagoas (UFAL), Rio Largo 57100-000, Brazil; igor.torres@ceca.ufal.br
* Correspondence: tiba@ufpe.br

Abstract: The objective of this work was to analyze the impacts on the transmission network due to the increase in centralized photovoltaic (PV) generators' incorporation. A study was carried out in a high-voltage (HV) transmission network, considering adjustments in the simulation environment for more realistic results. ANAREDE software and the static voltage stability evaluation method were used. The simulation was carried out in a steady state, considering an average load and the power of the PV generators corresponding to the base case (70.6 MW), with an increase of 100% of the predicted total (270 MW) for the future. The results showed that, under normal and contingency conditions, small disturbances caused voltage instability. It was observed that the incorporation of PV generators contributes to the improvement of the voltage stability in the bars close to their insertion. However, the greater the PV distribution and generation was, the greater the influence on the attenuations of the voltage profiles through the transmission system was.

Keywords: permanent regime; centralized photovoltaic generation; voltage variation

check for updates

Citation: Lobo, F.X.; de Negreiros, G.F.; Torres, I.C.; Tiba, C. Evaluation of Voltage Variations Arising from the Increase in Photovoltaic Insertion in the Transmission Network: Case Study Coremas-PB Power Plant. *Energies* **2023**, *16*, 7310. https://doi.org/10.3390/en16217310

Academic Editor: Theofilos A. Papadopoulos

Received: 9 September 2023
Revised: 11 October 2023
Accepted: 25 October 2023
Published: 28 October 2023

Copyright: © 2023 by the authors. Licensee MDPI, Basel, Switzerland. This article is an open access article distributed under the terms and conditions of the Creative Commons Attribution (CC BY) license (https://creativecommons.org/licenses/by/4.0/).

1. Introduction

Photovoltaic (PV) solar energy has established itself as a reality around the world from both the technical and commercial points of view. According to data from the International Energy Agency [1,2], by the end of 2022, there was approximately 1.2 TW of accumulated global installed capacity of solar PV energy, with about two-thirds coming from centralized generation. In Brazil, according to the National Electric Energy Agency [3], the share of hydroelectric generation in the energy matrix was 52.74% in June 2023. In the past, Brazilian hydroelectric plants represented up to 90% of the installed capacity [4]. These data highlight the growing importance of solar PV energy as an alternative and complementary source to hydroelectric generation in the global and national energy matrix. Brazil has excellent availability of solar energy resources [5], and, with the decline in the costs of photovoltaic equipment, solar photovoltaic (PV) energy is leveling its deployment costs with the prices of wind, hydroelectricity, and other renewable energy sources [6–8]. Consequently, the Brazilian government and electricity companies began to evaluate and consider photovoltaic plants in a centralized way, as a major contributor to the efficient diversification of the Brazilian electricity matrix.

According to the 2050 National Energy Plan, prepared by the Energy Research Company and based on MME guidelines, the total installed power of the centralized PV generation may exceed 100 GW by 2050, when considering restrictions on wind generation and problems with the expansion of transmission lines, a situation that would reduce generation from conventional sources [9,10]. Such considerations would estimate the share

of centralized solar PV to be between 18% and 30% of the total installed capacity of the system in 2050. Figure 1 shows the expansion of Brazilian electricity generation from renewable sources, for the period 2019–2029. Solar photovoltaic energy represents more than 30% of the total of this expansion, though little more than half is centralized [11].

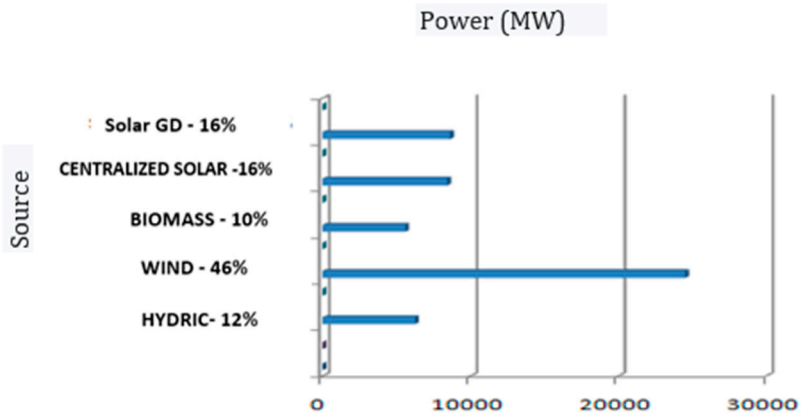


Figure 1. Expansion of installed capacity (MW) by 2029, with renewable sources. Source: [7].

Like wind generation, solar PV is stochastic, that is, it is not possible to determine, with certainty, the generation of energy in a future instant. So, stochastic intermittency, for example, the passage of a cloud, causes effects on the electricity transmission parameters of the electrical system. Another driving factor in the challenge to realize all solar PV energy is the need to accommodate the changing net load (normal load minus variable solar source generation) associated with high midday PV generation and the low-electricity-demand duck curve [12–14].

Large centralized PV systems, when inserted into the transmission network, cause phenomena and new challenges and, therefore, require specific studies [1]. For example, replacing conventional synchronous generators with photovoltaic generators can generate new stability problems, such as changes in voltage levels, the inversion of the standard transmission flow, reduced reactive support in the transmission network, and the reduced reliability of the transmission network in a contingency situation (the shutdown of a line or system equipment). These changes in the nominal operational condition of the system are permanent changes, that is, they are definitive in nature and need to be supported or adjusted by other sections of the electrical system so that they do not exceed the operational limits of the electrical network components [15,16]. These situations negatively impact the stability and reliability of the electrical system.

Therefore, large centralized PV systems, when inserted into the transmission network, cause phenomena and new challenges and, therefore, require specific studies, such as on the ideal levels of penetration of these sources and on the ability to control voltage levels when the demand is now supplied by this type of source [17].

2. Voltage Regulation Problems

2.1. Steady-State Voltage Variations

PV integration at various penetration levels can have a significant impact on transmission system bus voltages. It is necessary to know the magnitude of the changes in the steady-state voltage on electrical system buses to identify the most sensitive buses and avoid the adverse conditions that may occur with increases in PV penetration [5,18,19]. According to [16], the integration of PV systems can be beneficial as well as harmful, depending on their level of penetration and the point of interconnection.

Voltage stability is associated with the ability of the power system to maintain an adequate voltage profile, both under normal operating conditions and in the event of severe disturbances. According to [17], although the voltage instability phenomenon is a dynamic process, static analysis based on surveys of curves (P × V) and (V × Q),

which represent curves of active power (W) by voltage (V) and voltage (V) by reactive power (VAr), respectively, were internationally adopted to assess voltage stability. Figure 2 presents the results of simulations that used realistic models based on public data similar to real transmission systems, where the behavior of the voltage level for different buses of the simulated system is represented. The complete simulated system was composed of 2000 bars or nodes, which represent electrical connection points, and was part of the Texas region. The network consisted of three voltage levels (345/115/13.8 kV), and the system was designed with a peak demand capacity of 49.7 GW, while the maximum load could reach up to 28 GW.

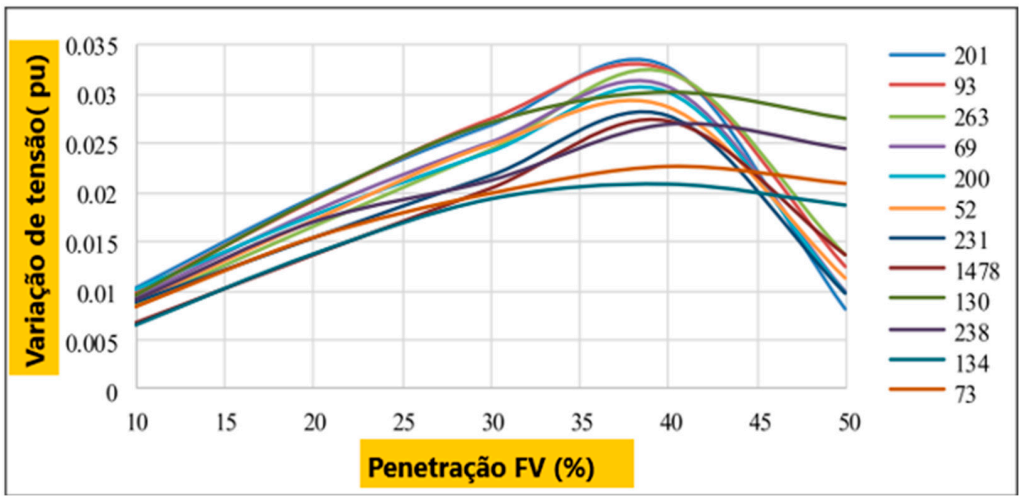


Figure 2. Voltage variation per bus of the simulated system, at different levels of PV penetration. Source: [5].

The voltage variations of the 115 kV bars of the simulated transmission system, with various levels of PV penetration, are shown in Figure 2 [12]. This type of voltage behavior is observed when more loads are being fed with the closest photovoltaic generation, leading to a less reactive power requirement from conventional generation, which is farther from the load centers [20]. After 40% PV penetration, the reverse flow of active energy occurs through the lines in the opposite direction of the loads, resulting in a constant increase in the reactive power flow and a decrease in the bus voltage magnitudes. Voltage instability is strongly associated with deficiency in system reactive support [20].

2.2. Modeling of Electrical Parameters in a Contingency Situation

Voltage stability assessment methods can be divided into static and dynamic methods. Static methods are based on the analysis of the systems of algebraic equations obtained from the power flow model. Dynamic methods, in general, are based on the time solutions of the systems of differential and algebraic equations representing the dynamic performance of system components [14,17,21].

The phenomenon of voltage instability can be initiated in two ways: first, there are large disturbances in the system caused, for example, by short circuits, transmission line shutdowns, etc. In this case, voltage instability can immediately manifest itself (within a few seconds) after the disturbance, similar to the problem of angular instability (transient voltage instability), or some time (several minutes) after the disturbance, through a voltage-degradation-profile slowdown (long-term voltage instability). Another reason would be small disturbances caused by normal load variation. This type of phenomenon is normally treated as a static voltage stability problem. Voltage instability caused by small disturbances, in turn, is associated with the limits of the maximum power transfer in the transmission system and insufficient reactive power generation in the affected area [16,21].

Although the phenomenon of voltage instability is essentially dynamic, static methods are important for their computational efficiency and for the information they produce regarding sensitivities, degrees of instability and stability margins. Static methods are suitable for studies related to instability caused by small disturbances, in which the main objective is to determine the maximum limits of the power transfer and reinforcements in the support of reactives, in order to increase these limits [14,17,21].

Power flow studies are carried out to verify the behavior of the electrical network in a steady state. According to [22], it is evaluated whether the voltage levels on the buses and the loads on the lines, transformers, and other components of the transmission network, for a given configuration of the electrical network and a given condition of load and generation, meet the criteria established in the Grid Procedures of the national system operator (ONS), in submodule 2.3. In the Brazilian system, users of the basic transmission network must meet the requirements of the voltage ranges that are classified according to criteria defined in the ONS Network Procedures, in submodule 2.3, through the voltage limits values that are applied to the most different levels, at the connection point, with reference to the values for high voltage, as expressed in Table 1.

Table 1. Admissible voltage between phases at 60 Hz. Source: the authors (2021).

Rated Operating Voltage	Normal Operating Condition		Operation Condition under Contingency	
(kV)	(kV)	(pu)	(kV)	(pu)
<230	-------	0.95 to 1.05	-------	0.90 to 1.05
230	218 to 242	0.95 to 1.05	207 to 242	0.90 to 1.05
345	328 to 362	0.95 to 1.05	311 to 362	0.90 to 1.05
440	418 to 460	0.95 to 1.046	396 to 460	0.95 to 1.046
500	500 to 550	1.00 to 1.10	475 to 550	0.95 to 1.10
525	500 to 550	0.95 to 1.048	475 to 550	0.90 to 1.048
765	690 to 800	0.90 to 1.046	690 to 800	0.90 to 1.046

Table 1 presents the voltage limits allowed for the ideal and safe operation of the electrical system under normal operating conditions and under contingencies, in accordance with the rules proposed by the National Electrical System Operator (ONS) for the coordination and control activities of the operation of the electrical system's generation and transmission of electrical energy, which are part of the National Interconnected System. Then, according to the nominal voltage level operated at a given point in the system, upper and lower limits would be allowed, at which the voltage could remain, in a permanent state, without compromising the system's operation. However, it is satisfactory that the voltage remains in a nominal condition, so there is always a margin available for possible changes in voltage. These changes in voltage levels occur in transmission networks due to an excess or a deficiency of reactants in the network.

It is possible to make changes to the electrical system's configurations, such as increasing the penetration of photovoltaic generation or removing regulatory equipment (contingencies), thus simulating small-scale disturbances. These parameter changes would be treated as a static voltage stability problem. Through scenarios, it is possible to identify the best conditions so that the system, even under the loss of stability, maintains satisfactory behavior in accordance with the required criteria.

3. Electric Network Modeling

3.1. Modeling of the Photovoltaic System in ANAREDE Software

Figure 3 illustrates the graphical representation of the simulation equipment, used to model the photovoltaic system in ANAREDE software, version 11.05.04. The photovoltaic plant (UFV) consists of two circuits, at 34.5 kV, for exclusive use, that connect to a 34.5/230 kV—120 MVA collector substation, called SE Rio Alto, shared between UFV Coremas I, UFV Coremas II, and UFV Coremas III, which connect to a 230 kV Chesf trans-

mission line, about seven kilometers and five hundred meters long, that, in turn, connects to the transmission system from the substation of Coremas-PB [23–25]. The PV generators are part of the Coremas-PB PV plant and are connected to the buses (RIOALTUFV032-5315 and RIOALTUFV009-7916) [23–25]. The representation of the PV generator is accomplished through the constant power model, that is, the model does not express the transition dynamics of the states of high or low solar incidence. So, as the ANAREDE program expresses the electrical system in a steady state, when it comes to the effect on the electrical parameters caused by the variation in solar generation, it is only possible to quantify it after each resolving interaction of the program.

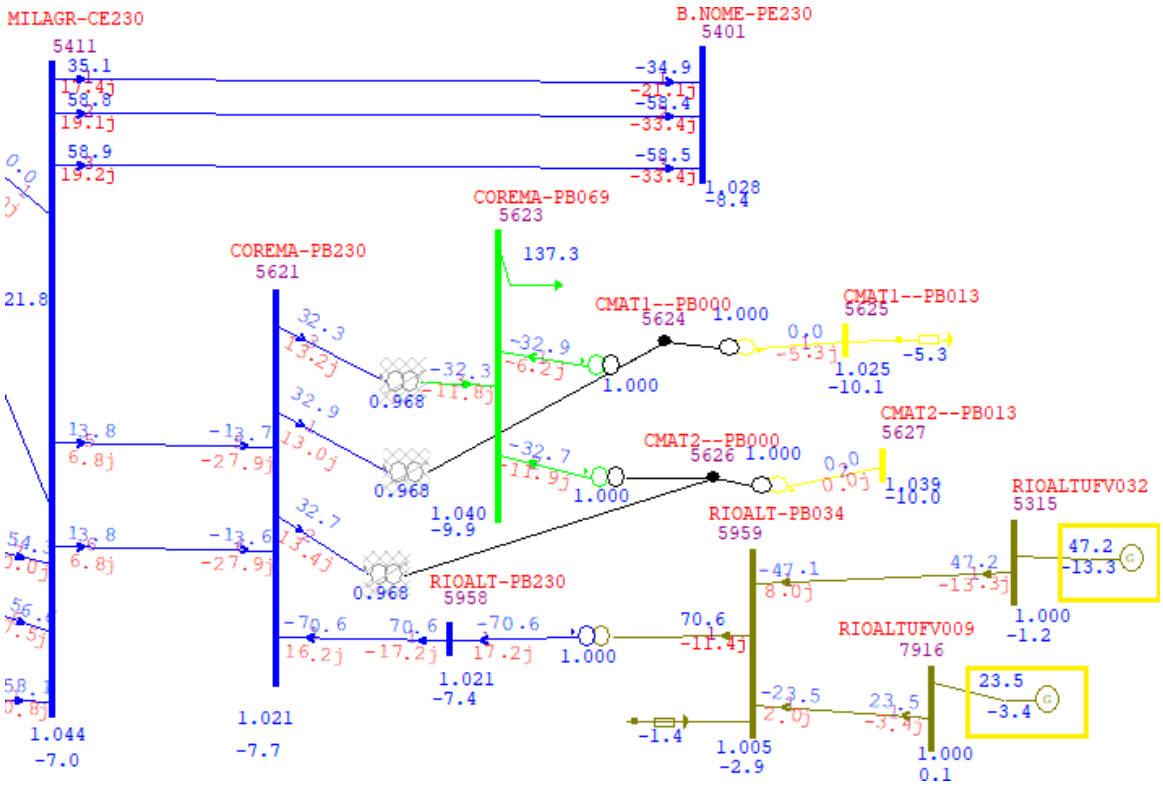


Figure 3. Diagram with section of the simulated system containing the PV generation. Source: the authors.

The power factor of the PV generators must be variable and follow the maximum and minimum reactive injection criteria, as defined in item 5.2 of submodule 2.10, contained in the ONS Grid Procedures [22,26].

A graphical representation of equipment, in the simulation, follows the standards of Network procedures and the color of circuit sections follow the Eletrobrás Chesf standard. The red color represents the circuit at voltage level 500 kV, the blue color represents the circuit at 230 kV, the green color represents the 69 kV voltage level, the color brown represents the 34.5 kV circuit and yellow represents the 1 kV circuit.

3.2. Transformer Modeling

The model used to simulate the transformer in ANAREDE, in the power flow calculation, was the positive sequence equivalent. However, it is important to emphasize that the power losses considered in this model are only reactive losses. In addition, the under-load tap changer can have continuous or discrete performance, depending on the specific configuration.

In the program version used in this simulation, the phase-shifting transformers have fixed angles, meaning there is no dynamic variation in these angles during the simulation process.

Table 2 presents the main transformers of the electrical circuit being studied, providing relevant information about their characteristics and parameters used in the modeling. These transformers play an essential role in the distribution and regulation of voltage throughout the electrical system, ensuring an adequate energy supply to the various points of consumption.

Table 2. System transformer input data.

Transformer	R (%)	X (%)	B (Mvar)	Capacity (Mva)	Transformation Ratio
5408 (MILAGR-CE500)–5411 (MILAGR-CE230)	0	0.096	0	600	500/230 kV
5621 (COREMA-PB230)–5623 (COREMA-PB069)	0	13.19	0	100	230/69 kV

Source: [4].

It should be noted that the proper choice of transformers and the correct representation of their characteristics are essential to obtain accurate and reliable results in the electrical studies carried out using ANAREDE.

3.3. Transmission Line

Transmission lines (LT) have four parameters that play an important role in their operation and, consequently, in the energy transport capacity. These parameters are resistance (R), series reactance (X), conductance (G), and shunt susceptance (B) [5,14,27]. However, conductance is usually neglected, since its effect on the line is considered very small in relation to that of the other parameters [5,17].

Table 3 presents the main transmission lines of the electrical circuit being studied, providing relevant information about these parameters and the capacity of each line.

Table 3. Transmission line parameters.

Transmission Line	R	X	B	Capacity
	(%)	(%)	(MVAr)	(MVA)
5428 (QUIXAD-CE500)–5408 (MILAGR-CE500)	0.26	2.97	399.02	2070
5050 (L.GONZ-PE500)–5740 (OLINDI-BA500)	0.31	3.1	324.34	1306
5001 (P.AFONS-BA500)–5740 (OLINDI-BA500)	0.21	2.68	272.76	2165
6300 (SOBRAD-BA500)–5050 (L.GONZ-PE500)	0.29	3.99	411.44	2165
5050 (L.GONZ-PE500)–5408 (MILAGR-CE500)	0.21	2.57	343.26	2186
6500 (JUAZEI-BA500)–5050 (L.GONZ-PE500)	0.25	3.2	327.32	1732
6640 (CURRAL-PI500)–5408 (MILAGR-CE500)	0.155	2.231	356.98	1992
5570 (S.J.PI-PI500–6640 (CURRAL-PI500)	0.134	1.92	279.9	1992
5577 (SJ-SB2CAP500)–6300 (SOBRAD-BA500)	0.153	2.272	327.32	1732
6300 (SOBRAD-BA500)–6500 (JUAZEI-BA500)	0.04	0.48	47.043	2165
6500 (JUAZEI-BA500)–5050 (L.GONZ-PE500)	0.25	3.2	327.78	2165
5411 (MILAGR-CE230)–5621 (COREMA-PB230)	2.2	11.64	20.3	291
5411 (MILAGR-CE230)–5401 (BOM NOME-PE230	1.09	4.83	25.02	400
5621 (COREMA-PB230)–5958 (RIOALT-PB230)	0.1466	0.7	1.287	210

Source: [4].

The series resistance and reactance influence the active and reactive power losses along the line, while the shunt susceptance influences the magnetization currents. These parameters are crucial to guarantee the adequate transmission of electric energy in an efficient and safe way [28].

It is important to emphasize that the correct modeling and consideration of the transmission line parameters are essential to obtain accurate and reliable results in the electrical studies carried out using ANAREDE, allowing for the evaluation of the performance of the electrical system and the identification of possible critical points or needs for reinforcement in the transmission network.

3.4. System Description

The electrical parameters of the simulated system equipment were previously presented in Sections 3.1, 3.2 and 3.3, addressing their specific characteristics. In this subsection, the focus is on the main circuits of the northern section of the Eletrobrás-Chesf system being studied. The electrical data from part of this system are graphically presented, aiming a clear and simplified representation.

Figures 4 and 5 illustrate the electrical characteristics of the transmission network modeled in the ANAREDE program through a single-line diagram. In this diagram, we can identify the Coremas substation, together with the adjacent substations, the transmission lines that connect them, and the conventional generators present in the studied section. It is noteworthy that the circuit in question is composed by a total of 11 transmission lines of 500 kV, 3 transmission lines of 230 kV, and 15 buses. Of these buses, eight have voltage levels of 500 kV, three are 230 kV, one is 69 kV, and three are 34 kV.

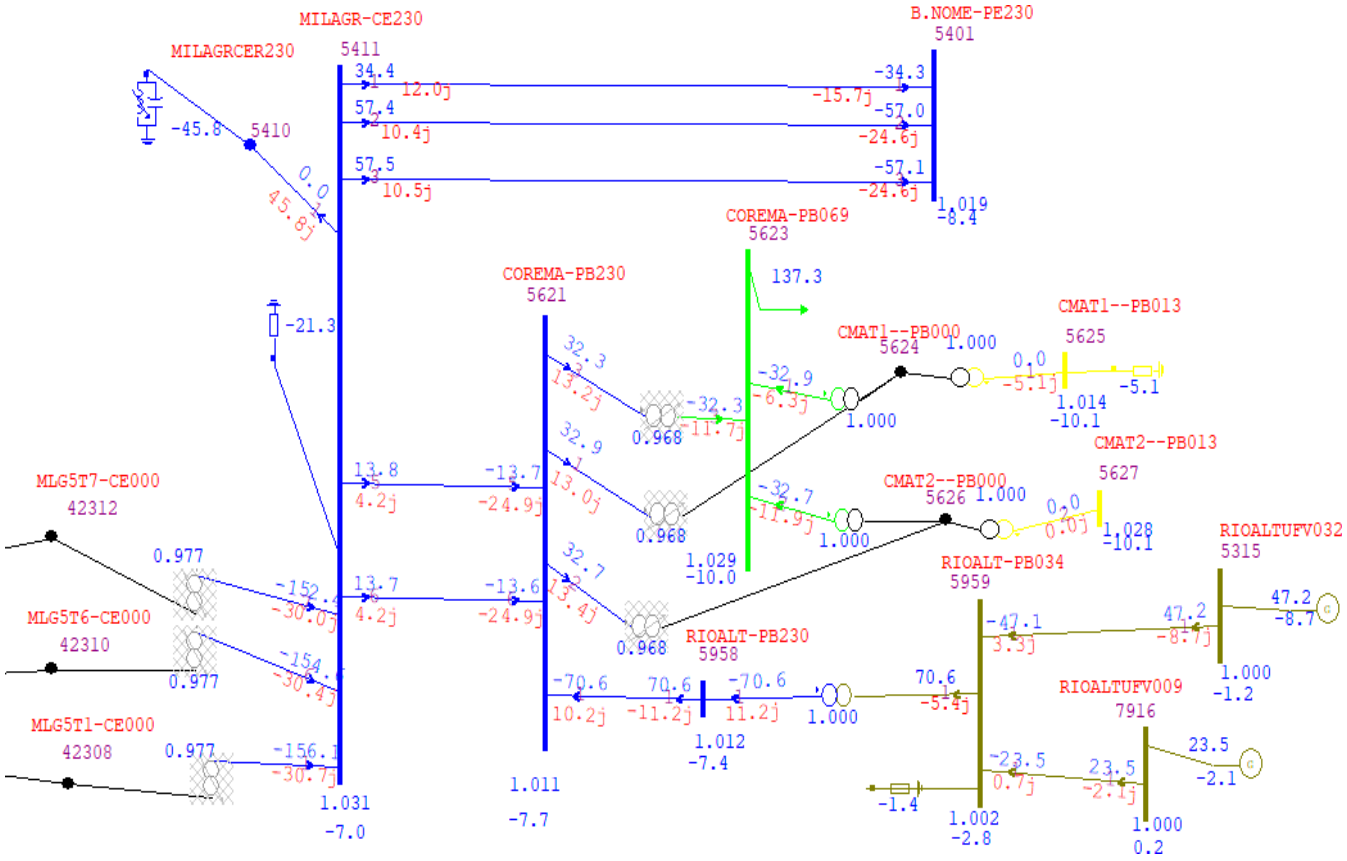


Figure 4. Simplified single-line diagram of the Section 1 system. Source: the authors.

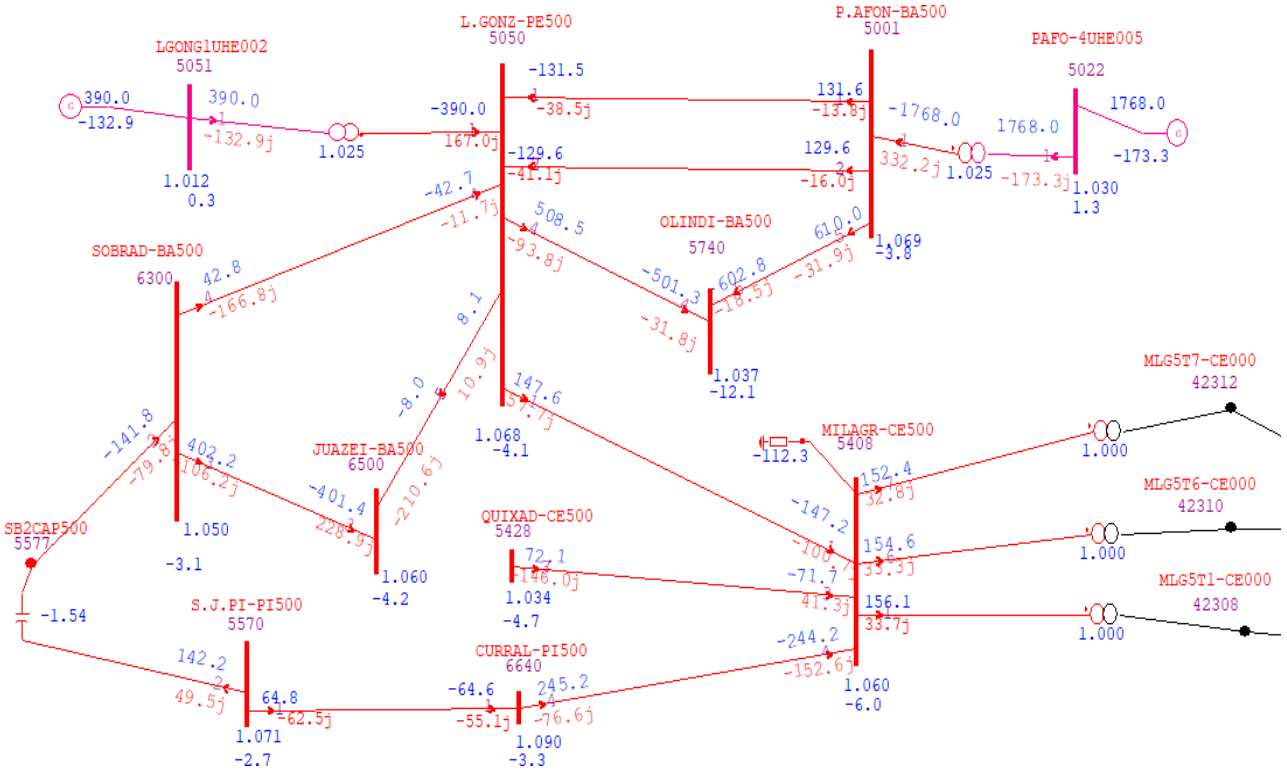


Figure 5. Simplified single-line diagram of the Section 2 system. Source: the authors.

Among the equipment present in the system, there are devices responsible for controlling the power flow in the electrical network. They are three transformers with a transformation ratio of 500/230 kV, three 230/69 kV transformers, a 500 kV shunt reactor, a 230 kV static compensator, and a 230 kV shunt reactor. It is important to highlight that all loads connected to the electrical grid under study were modeled with constant power, and the photovoltaic system was modeled as a generation equivalent and was connected to the bus (5621 COREMAPB-230), injecting active and reactive power.

This detailed representation of the equipment and characteristics of the electrical system allows for a more accurate analysis of the power flow, stability, and other relevant aspects of this study. The correct modeling of control devices and the consideration of the characteristics of the loads and the photovoltaic system are essential to obtain reliable results and support decision making within the scope of the operation and the planning of the electrical network.

4. Methodology

The electrical parameters provided by ONS and loaded into the ANAREDE program, version 15.5.4, were used. The power flow was performed using the Newton–Raphson method (NEWT tool from ANAREDE). The data loaded into the program represent all the parameters of the system's equipment and also the average generation and load profile associated with the average load level of the electrical system, for the month of January, 2021. Electrical data for part of the northern Eletrobrás-Chesf system were graphically represented, as shown in Figures 4 and 5, with the aim of verifying the behavior of voltage levels in the bars of the high-voltage electrical system, for contingency situations.

The generation data provided by the ONS are average data, that is, data that do not portray a maximum generation from the photovoltaic plant at a given time of day. For the simulations, PV generation data with a "maximum" power injection level at certain times of the day were considered; that is, instantaneous data were loaded into the program so that it was possible to carry out the simulation with maximum generation characteristics. For

the base case, generation data for the month of January were considered, which historically is the month with the highest PV generation.

For the initial case, the system was simulated for a maximum active power generation value of 70.6 MW, minimum reactive power of −23 MVAr, and maximum power of +23 MVAr, according to the criteria defined in the ONS Network Procedures, in its submodule 2.10, which requires generation agents to connect to the basic transmission network. The Coremas PV plant was modeled with equivalent generation directly linked to SE-Coremas, with an active power generation of 70.6 MW. However, as already granted by regulatory agents, an increase in total generation was approved, and, due to this, the contribution of the PV complex was also simulated, considering an increase of 100% of the total expected to be expanded, that is, a maximum generation of 270 MW.

4.1. Description of Scenarios and Results

4.1.1. Scenario 1 (Baseline)—Actual Transmission System with Current Photovoltaic Generation

In this scenario, the average load level electrical system data were loaded. The base case data were for the month of January, since historically it is the month with the highest PV generation for the studied region. All load and generation data are average data within the time defined for the average load level of the electrical system; therefore, an adjustment was made to the PV generation data through SUPERVISION software, where it was possible to reach the maximum generation in MW time of this PV plant for the month of January 2021. The graphical representation of the real system under analysis, defined as the base case, is divided into two sections, represented in Figures 6 and 7—with the contribution of power from the photovoltaic generators RIOALTUFV032-5315 and RIOALTUFV009-7916—with the objective of verifying the behavior of the high-voltage electrical system, as well as forming, through the obtained results, a reference base case for later comparisons.

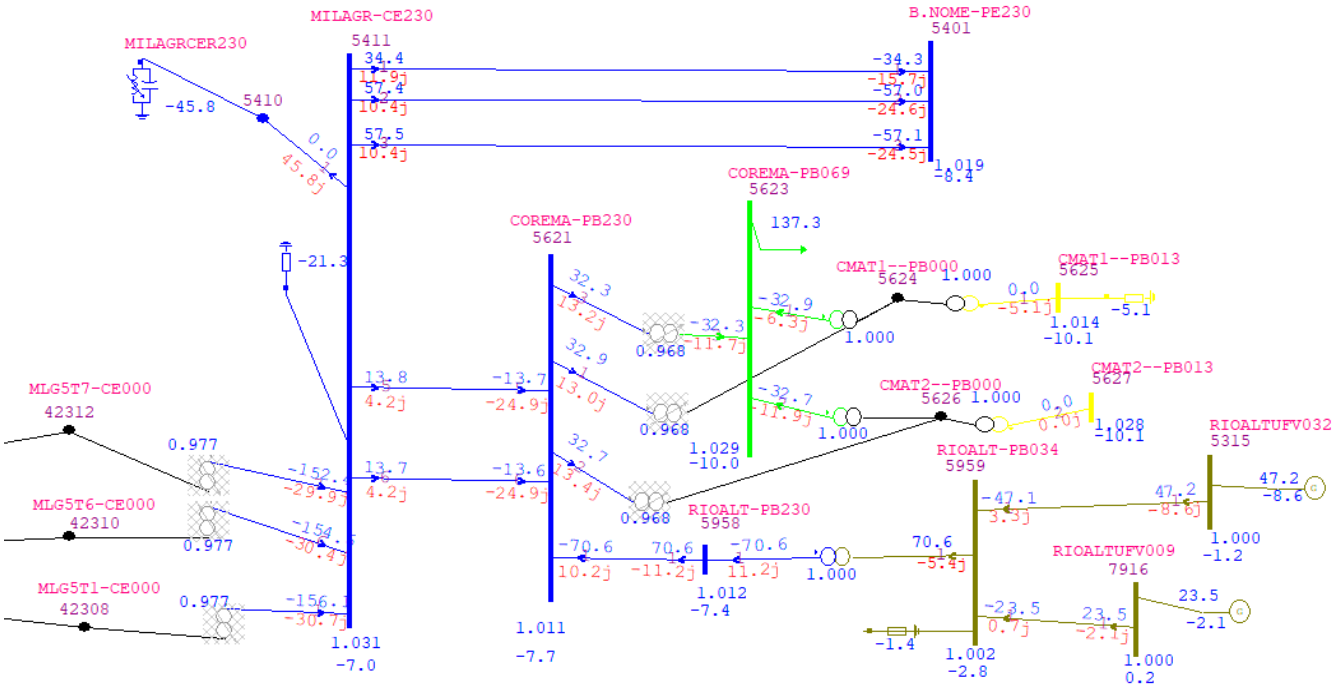


Figure 6. Excerpt 1 of the real electrical system (base) modeled and simulated in ANAREDE software. Source: the authors.

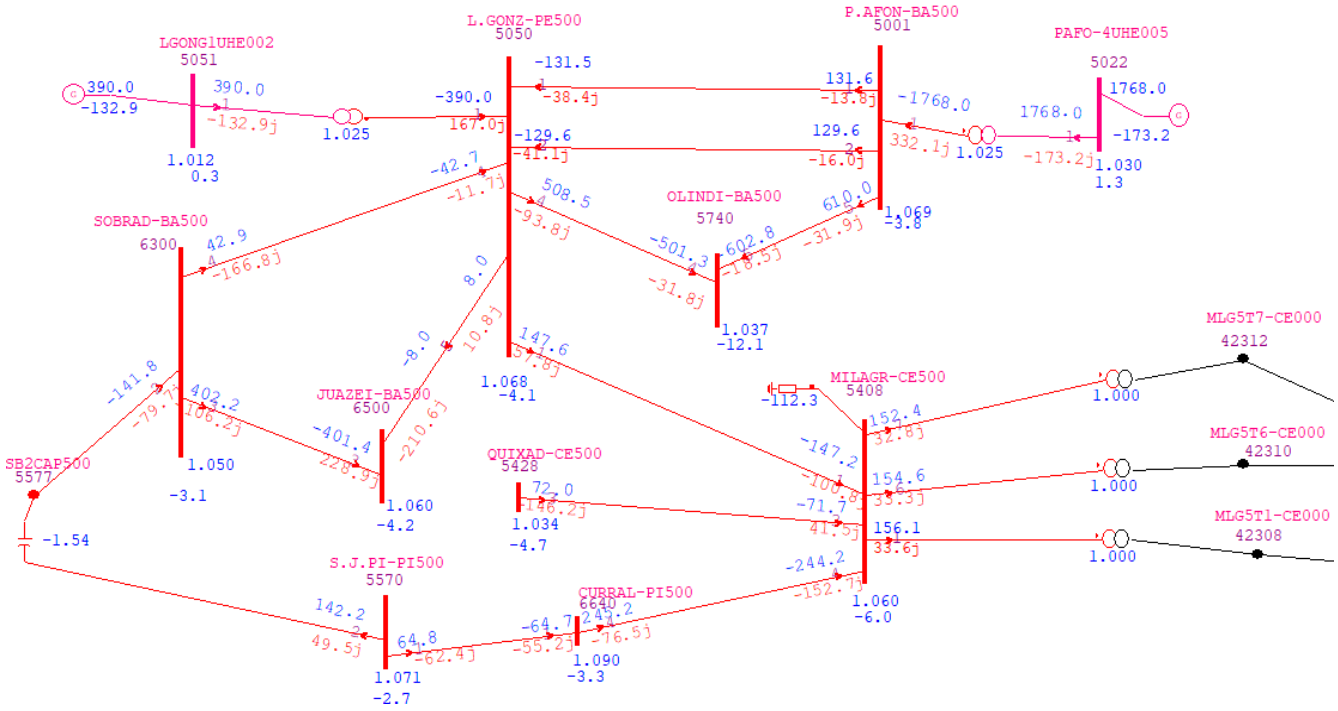


Figure 7. Section 2 of the real electrical system (base) modeled and simulated in ANAREDE software. Source: the authors.

To analyze the voltage levels of the selected buses, Table 4 presents the main data that were extracted from the output report after executing the power flow from the base case data proposed for scenario 1.

Table 4. Consolidated data from the stress report for scenario 1.

Bars	Module	Angle	Generation		Load		Static C.	Shunt	Type	Status
	(pu)	(°)	(MW)	(MVAR)	(MW)	(MVAR)	(MVAR)	(MVAR)		
5621 (COREMA-PB230)	1.011	−7.7	0	0	0	0	0	0	PQ	On
5411 (MILAGR-CE230)	1.031	−7	0	0	0	0	−46.3	−21.3	PQ	On
5401 (BOM NOME-PE230)	1.019	−8.4	0	0	0	0	0	0	PQ	On
5959 (RIOALT-PB034)	1.002	−2.8	0	0	0	0	0	−1.4	PQ	On
5408 (MILAGR-CE500)	1.060	−6	0	0	0	0	0	−112.3	PQ	On
5050 (L.GONZ-PE500)	1.068	−4.1	0	0	0	0	0	0	PQ	On
5001 (P.AFON-BA500)	1.069	−3.8	0	0	0	0	0	0	PQ	On
5623 (COREMA-PB069)	1.029	−10	0	0	137.3	29.9	0	0	PQ	On

Source: the authors (2021).

The operating state with some parameters of the bars selected for analysis, obtained from the output report generated in the load flow solution for the first case, can be seen in Table 4. The automatic TAP controls (voltage regulation) of two groups of transformers were inhibited in order to emphasize the PV contribution, so there could be a better comparison between the simulation scenarios.

4.1.2. Scenario 2—Actual Transmission System with Photovoltaic Generation with 50% of the Expected Increase in Active Power Generation

In this scenario, the same electrical data as the base case were considered, and a 50% increase was made in the total generation expected to come into operation in the photovoltaic system, which has a capacity of 270 MW, as detailed in Section 4. For scenario 2, a new active generation (MW) value for the photovoltaic complex was defined, which was adjusted to 170 MWac. Furthermore, the reactive power insertion limit (MVAr) of the

photovoltaic complex was adjusted to 55 MVAr. This PV generation value was defined as an intermediate value between the minimum generation (already in operation) and maximum generation (total generation expected to come into operation and already granted). With scenario 2, it is possible to evaluate the behavior of the parameters being studied on an intermediate PV insertion scale.

This change in the reactive power limit was carried out with the objective of maintaining the power factor of the photovoltaic plant within the range of 0.95, both inductive and capacitive, as established in submodule 3.2 of the Grid Procedures. This restriction aims to ensure that bus 5959 (RIOALT-PB034), to which the photovoltaic plant is connected, maintains a nominal voltage close to 1 pu (unit per unit).

As part of this adjustment, the automatic TAP controls (voltage regulation) of two groups of transformers were inhibited. This decision aimed to highlight the contribution of the new configuration, with the increase in photovoltaic generation to maintain stability and an adequate level of voltage in the electrical grid.

By carrying out these modifications and adjustments, it is possible to evaluate the resulting impacts on the electrical system, analyze voltage stability, verify power flow, ensure compliance with established operational and regulatory requirements, and verify the possible contribution of PV systems in reducing operational regimes of regulation equipment. These considerations are essential for the correct integration and operation of the photovoltaic complex in the context of the electrical grid under study.

- 5408 (MILAGR-CE500)—5411 (MILAGR-CE230),
- 5621 (COREMA-PB230)—5623 (COREMA-PB069).

The data analyzed were the change in bus voltage levels on the following buses:

- 5621 (COREMA-PB230);
- 5411 (MILAGR-CE230);
- 5401 (BOM NOME-PE230);
- 5959 (RIOALT-PB034);
- 5623 (COREMA-PB069);
- 5408 (MILAGR-CE500), which are buses close to the PV connection and in the buses;
- 5050 (L.GONZ-PE500) and 5001 (P.AFON-BA500), which are buses close to the conventional generation (hydroelectric).

According to data extracted from the program's output report, after the adaptations foreseen for scenario 2, some parameters can be extracted from the bars selected for analysis. The operating status of the buses for scenario 2 can be seen in Table 5.

Table 5. Consolidated data from the stress report of scenario 2.

Buses and PV Generators	Module	Angle	Generation		Load		Shunt	Type	Status
	(pu)	(°)	(MW)	(MVAR)	(MW)	(MVAR)	(MVAR)		
5621 (COREMA-PB230)	1.09	−11.3	0	0	0	0	0	PQ	On
5411 (MILAGR-CE230)	1.032	−13.9	0	0	0	0	−21.3	PQ	On
5401 (BOM NOME-PE230)	1.020	−15.7	0	0	0	0	0	PQ	On
5959 (RIOALT-PB034)	0.994	0.6	0	0	0	0	−1.4	PQ	On
5408 (MILAGR-CE500)	1.061	−13	0	0	0	0	−112.3	PQ	On
5050 (L.GONZ-PE500)	1.074	−12.3	0	0	0	0	0	PQ	On
5001 (P.AFON-BA500)	1.073	−11.9	0	0	0	0	0	PQ	On
5623 (COREMA-PB069)	1.027	−13.6	0	0	137.3	29.9	0	PQ	On

Source: the authors (2021).

After analyzing the results of scenario 2, some conclusions can be observed regarding the effects of photovoltaic (PV) generation on the bus voltages of the electrical system under study.

In the buses closest to the PV plant, such as buses 5621 (COREMA-PB230), 5623 (COREMA-PB69), and 5959 (RIOALT-PB034), a small reduction in voltage levels was

identified when compared to scenario 1. This reduction can be attributed to the insertion of PV generation in the grid, which causes an impact on the voltage of the closest bars.

In contrast, in buses located at a greater distance from the PV generation, which are separated by long transmission lines, such as buses 5411 (MILAGR-CE230), 5401 (BOM NOME-PE230), and 5408 (MILAGR-CE500), there was practically no significant variation in voltage. This is because the influence of PV generation decreases as the distance between the bus and the PV plant increases. As for buses 5050 (L.GONZ-PE500) and 5001 (P.AFON-BA500), which are closer to conventional generation, an increase in voltage levels was observed. This rise was more pronounced as the bar approaches conventional generation. This behavior is the result of the combination of the effects of PV and conventional generation on the power grid.

To graphically visualize these effects, Figure 8 presents a graph that illustrates the voltage variations in the bars of the analyzed section. The bars are organized from top to bottom, in order of proximity to the PV plant, allowing for a clear visualization of voltage variations along the network.

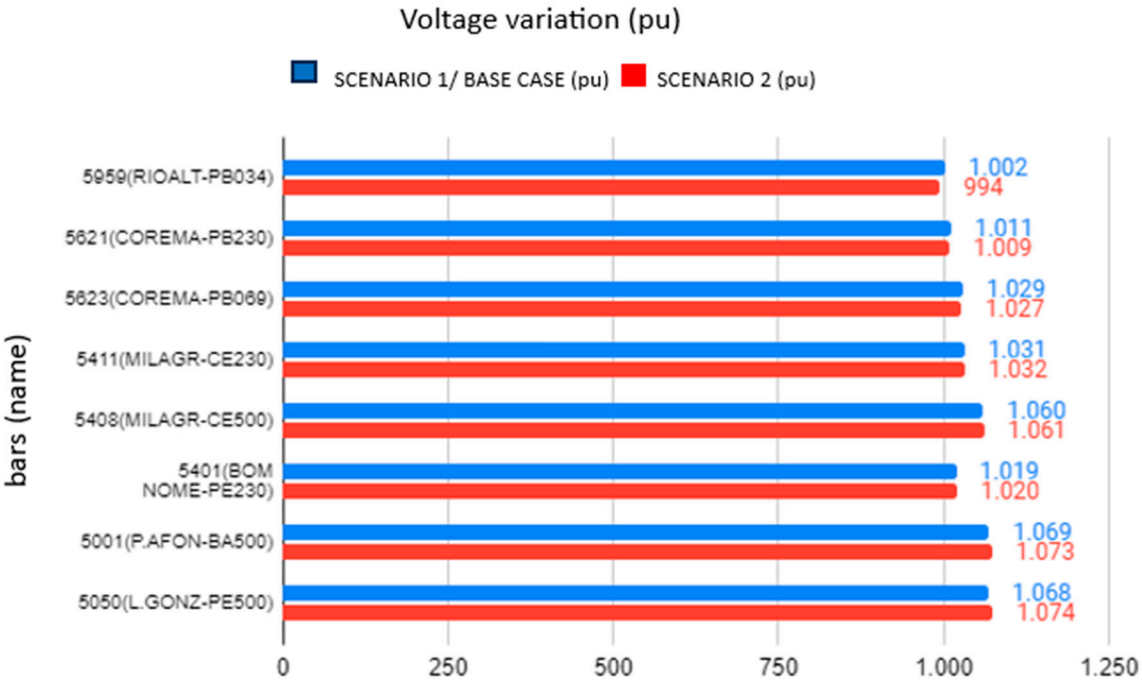


Figure 8. Voltage variation for the studied buses, comparing scenario 1 and scenario 2. Source: the authors (2021).

This information is essential to understand the impact of photovoltaic generation on the electrical system, assess voltage stability, and take appropriate measures to ensure the good performance and safe operation of the system. The analysis of the effects of PV generation on bus voltages provides important insights for the efficient planning and operation of the electrical grid.

Figure 8 graphically shows the PV effect in the analyzed section, in relation to voltage variation. The data shown in Figure 8 illustrates the voltage variations in bars, organized top to bottom, in order, from closest to furthest to the PV plant.

With the increase in photovoltaic (PV) generation defined for scenario 2, a voltage drop was observed in the buses close to the PV plant. This voltage reduction in the buses is caused by the increase in the reactive flow in this region, due to the increase in the active power generated by the PV plant. To control this increase in reactive power and mitigate voltage drops, PV generators began to supply reactive power, reducing the flow of reactive power from other parts of the system that could cause greater voltage drops.

In contrast, other buses closer to the traditional generation showed a slight increase in voltage, even with the decrease in the active power supplied by this conventional generation, since there was effective control of the reactive power flow from the synchronous generators. Bus 5959 (RIOALT-PB034), where the PV plant is connected and which has a voltage level of 34 kV, is worth highlighting. A more significant initial voltage drop was observed in this bus. This occurs due to the fact that lower-rated voltage transmission lines have a low susceptance (shunt parameter), making them very sensitive to the flow of active power. In this case, the additional contribution of active power from PV generation more intensely impacted voltages. However, the PV system can mitigate this voltage drop effect by controlling the reactive power in the bus, seeking to maintain the voltage close to appropriate levels.

As in scenario 1, no extrapolations of voltage limits were identified in scenario 2. It was possible to obtain more favorable voltage profiles, close to 1 pu (per unit), which indicates proper operation of the electrical system and better power quality for the energy supply. These analysis and observations make it possible to understand the effects of PV generation on bus voltages, identify critical points, and take measures to ensure the stability and proper performance of the electrical system. It is essential to consider these aspects when planning and operating systems with high penetration of photovoltaic generation, aiming at optimizing and securing the electrical network.

4.1.3. Scenario 3—Actual Transmission System with Photovoltaic Generation with 100% of the Expected Increase in Active Power Generation

In this scenario, a 100% increment of the total PV generation expected to come on stream is added to the base case. The new input value for active generation (MW) of the PV plant is 270 MWac. As accomplished in scenario 2, the reactive power insertion limit (MVAr) of the PV plant was also adjusted to a value of 80 MVAr. The change in the reactive power limit must be made to keep the power factor of the PV plant within the range of 0.95, inductive or capacitive, as defined in submodule 3.2 of the Grid Procedures.

As in scenario 2, the automatic tap controls of two groups of transformers were also frozen:

- 5408 (MILAGR-CE500)—5411 (MILAGR-CE230),
- 5621 (COREMA-PB230)—5623 (COREMA-PB069).

The same subcases that were analyzed in scenario 2 were analyzed, though with the new value of active and reactive power generation of the PV plant. According to the output report, generated from the new configuration defined for scenario 3, some parameters can be extracted from the buses selected for analysis. The operating status of the buses for scenario 3 can be seen in Table 6.

Table 6. Consolidated data from scenario 3 stress report.

Buses	Module	Angle	Generation		Load		Shunt	Type	Status
	(pu)	(°)	(MW)	(MVAR)	(MW)	(MVAR)	(MVAR)		
5621 (COREMA-PB230)	0.991	−4.7	0	0	0	0	0	PQ	On
5411 (MILAGR-CE230)	1.028	−10.9	0	0	0	0	−21.1	PQ	On
5401 (BOM NOME-PE230)	1.017	−12.8	0	0	0	0	0	PQ	On
5959 (RIOALT-PB034)	0.972	15.3	0	0	0	0	−1.3	PQ	On
5408 (MILAGR-CE500)	1.059	−10.2	0	0	0	0	0	PQ	On
5050 (L.GONZ-PE500)	1.074	−9.9	0	0	0	0	0	PQ	On
5001 (P.AFON-BA500)	1.073	−9.4	0	0	0	0	0	PQ	On
5623 (COREMA-PB069)	1.008	−7.1	0	0	137.3	29.9	0	PQ	On

Source: the authors (2021).

When comparing with scenario 3, it is possible to draw some conclusions regarding scenario 1. In the buses where the photovoltaic plant is closer, such as buses 5621 (COREMA-PB230), 5623 (COREMA-PB69), and 5959 (RIOALT- PB034), an even greater reduction in voltage levels was observed compared to scenario 2. This more pronounced reduction was a

result of the increase in photovoltaic generation at these points. On the other hand, in buses closer to photovoltaic generation, but separated by long transmission lines, such as buses 5411 (MILAGR-CE230), 5401 (BOM NOME-PE230), and 5408 (MILAGR-CE500), contrary to scenario 2, an increase in tension levels was observed. This change occurred due to several factors, such as the configuration of the electrical network and the distribution of reactive power flow from photovoltaic generators. In the case of buses 5050 (L.GONZ-PE500) and 5001 (P.AFON-BA500), which are closer to conventional generation, an increase in voltage levels was evidenced in comparison with the base case. However, regarding scenario 2 (with a 50% increase in PV generation), there were no significant changes.

For a clear visualization of these variations, Figure 9 presents the data of voltage variations in the buses, organized top to bottom in increasing order of proximity to the photovoltaic plant. These data allow for comparison among the three studied scenarios, providing valuable information about the effects of PV generation on the grid voltages. These comparative analyses are important to assess the impacts of photovoltaic generation in different scenarios and to identify the challenges and opportunities associated with the integration of this type of generation into the electrical grid. This information is essential for the efficient planning and operation of the electrical system, seeking to guarantee the stability, quality, and reliability of the energy supply.

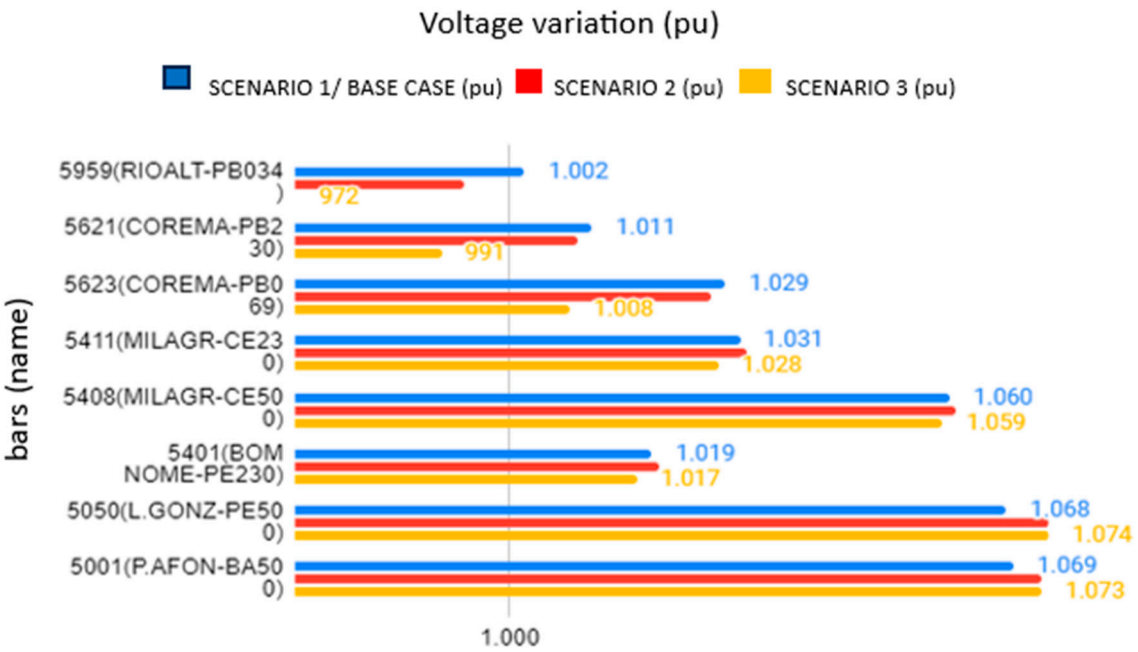


Figure 9. Voltage variation data on specific bars for scenarios 1, 2, and 3. Source: the authors (2021).

In scenario 3, which showed a greater increase in photovoltaic generation compared to scenario 2, a more significant drop was observed in the voltages of the buses closer to the photovoltaic plant. This voltage reduction on the buses was caused by the increase in the reactive power flow consumed by the series reactance of the transmission lines in this region, due to the increase in the active power generated by the PV plant in greater quantity.

As in scenario 2, the need for reactive power in this region of the system was largely met by photovoltaic generators, which began to supply reactive power and reduce the flow of reactive power from other parts of the system, avoiding more pronounced voltage drops.

In contrast, unlike what happened in scenario 2, other buses closer to the traditional generation showed a reduction in voltage, even with an even greater decrease in the active power supplied by this conventional generation. This occurred due to the significant increase in generation from the photovoltaic plant, which generates a reverse flow of active energy through the lines in the opposite direction to the closest loads, resulting in a constant

increase in the flow of reactive power consumed by the series reactance of the lines and in the reduction in the voltage magnitude on the buses.

Regarding the buses closer to traditional generation, such as hydroelectric plants, the voltage level of scenario 2 was maintained, even with the significant increase in photovoltaic generation. This stability can be explained by the effective control of reactive power performed by conventional generators, which maintain voltage levels to avoid significant drops in the buses due to the reduction in active power transport, being locally compensated by photovoltaic generators.

Another highlight in the initial comparison is bus 5959 (RIOALT-PB034), which has a voltage level of 34 kV and is where the photovoltaic plant is connected. A more relevant voltage drop was observed in this scenario compared to scenario 2. This can again be explained by the model of lower voltage transmission lines, such as those of 34 kV, which showed a more significant increase in active power when connecting the photovoltaic plant at bus 5959 (RIOALT-PB034). As in scenarios 1 and 2, no extrapolations of voltage limits were identified in this scenario.

These comparative analyses provide valuable insights into the effects of photovoltaic generation on the bus voltages of the electrical system, allowing for a deeper understanding of system behavior and assisting in planning and operating decisions. It is essential to consider these aspects to guarantee the stability, security, and quality of the electricity supply.

4.1.4. Scenario 4—Contingency Analysis with Minimum PV Generation

For scenario 4, the steady-state contribution of the PV system was simulated within the limits of current electricity generation (maximum injection of 70.6 MW of active power and 23 MVar of reactive power), under normal operating conditions and in contingency. The contingency occurred with the shutdown of shunt reactor 5408 (MILAGR-CE500), which is connected to the 500 kV miracle bus, and static compensator 5410 (MILAGRCER230), which is connected to the 230 kV miracle bus. The single-line diagram represented by Figure 10 shows the system equipment that is turned off, which is highlighted in green, and also the PV generators, which are highlighted in yellow.

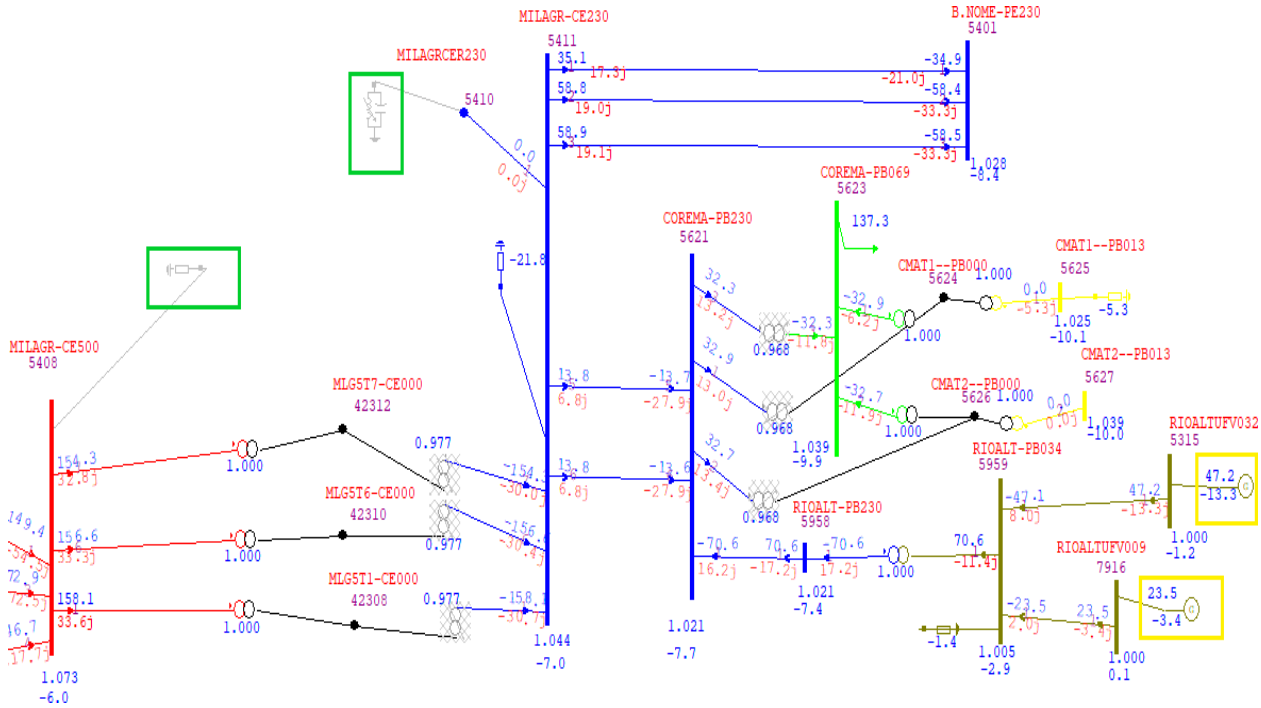


Figure 10. Excerpt from the real electrical system modeled and simulated in ANAREDE software. Source: the authors.

As previously mentioned, the removal of the shunt reactor of 5411 (MILAGR-CE230) and the static compensator of 5410 (MILAGRCER230) was simulated. These two pieces of equipment control a good part of the reactor in the section where the PV plant under study is directly inserted. For the first scenario, the influence of PV generation on the energy parameters in the base case condition was analyzed, that is, in the current generation condition before and after the described contingencies. For each proposed scenario, it was possible to verify and analyze changes in the voltage levels of the following buses:

- 5621 (COREMA-PB230);
- 5411 (MILAGR-CE230);
- 5401 (BOM NOME-PE230);
- 5959 (RIOALT-PB034);
- 5623 (COREMA-PB069);
- 5408 (MILAGR-CE500), which are buses closer to the PV connection; and on the bars:
- 5050 (L.GONZ-PE500) and 5001 (P.AFON-BA500), which are buses closer to conventional hydroelectric generation.

Voltage levels were compared in the selected buses for non-contingency conditions (with the regulation equipment connected to the system) and the contingency situation (loss of regulation equipment). Figure 11 presents a comparative graph of voltage growth in all buses verified in this study, with emphasis on the two COREMAS buses (5621 and 5623).

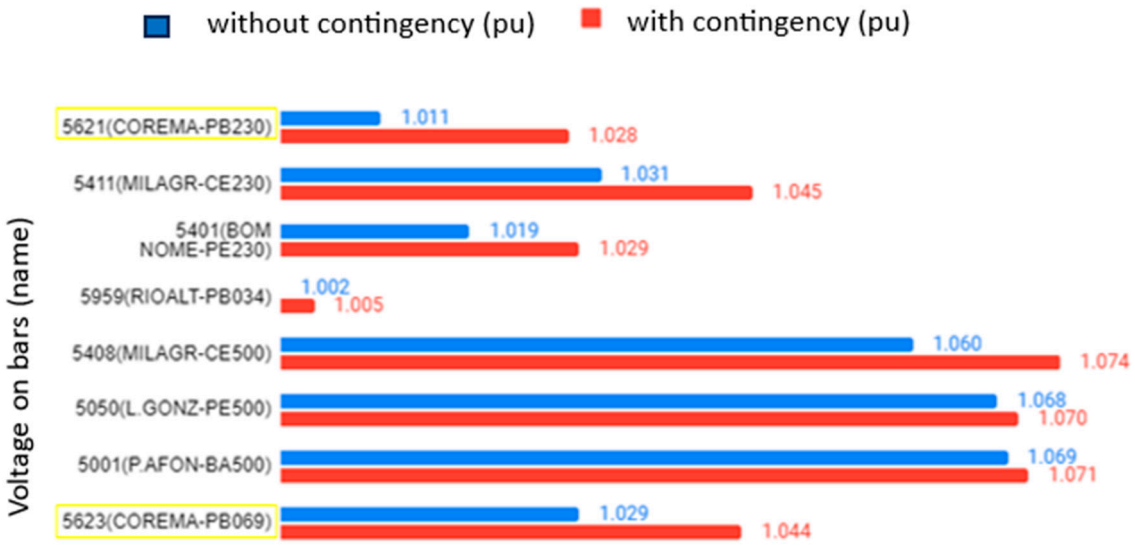


Figure 11. Quantitative representation of the stress levels per bar before and after the contingency under the conditions provided for the first case (base case). Source: the authors.

It is possible to verify that there was an increase in the voltage levels in the buses related to the scenario without contingency, caused by the removal of the reactive control equipment. There was a significant increase in the voltage levels of buses 5621 (COREMA-PB230) and 5623 (COREMA-PB069), increasing the voltage from 1011 pu to 1028 pu and from 1029 pu to 1044 pu, respectively. These two buses make up SE-COREMAS, to which the PV plant is connected, where there was a significant increase in voltage, which has a normative upper limit of 1.05 pu.

All buses had an increase in voltage level when the system lost the two control devices. At points furthest from the control elements and closer to traditional generation (hydroelectric), such as buses 5050 (L.GONZ-PE500) and 5001 (P.AFON-BA500), there was virtually no voltage variation. At the points closest to the reactive control elements and away from the generators, such as bus 5408 (MILAGR-CE500), there was a significant voltage variation, changing from 1.06 pu to 1074 pu. This voltage increase was expected due to the removal of the shunt reactor of 5411 (MILAGR-CE230) and the static compensator of

5410 (MILAGRCER230), which are reactive control elements in the transmission system and reactants are absorbed in the simulated condition.

The reactive absorption results in a steady-state voltage drop, since it increases the reactive flow along the LTS. In the transmission system, the electrical voltage is very sensitive to the flow of reactive power. Then, an increase in reactive transport causes a voltage drop across the LTS terminals. Another highlight would be bus 5959 (RIOALT-PB034), which has a voltage level of 34 kV and is where the PV plant is connected. This bus had a small voltage variation in steady state, changing from 1002 pu to 1005 pu. We can attribute these voltage increases in the buses furthest from the traditional generation to the reactive flow through the LTS that interconnect the referred buses, which decreased with the removal of equipment that absorbs reactives in the system.

Another factor would be the characteristic of LTS when carrying active power below its transmission capacity, which is the case of the lines that connect the bus closer to the PV generation to the system, contributing to the supply of reactive to the system and reducing the flow of reactive coming from the network, which results in an increase in bus voltage. This contribution is due to the LTS model with high voltage levels such as 230 kV and 500 kV, presenting high susceptance values in their shunt parameter.

So, if the flow of reactive from the generation towards the bus is lower, there is an increase in the voltage on these buses. If the bus is very closer to generation, which it reactively controls, its voltage modules have smaller variations in steady state, as is the case with buses 5050 (L.GONZ-PE500) and 5001 (P.AFON-BA500). Despite the 5959 bus (RIOALT-PB034) having a voltage level of 34 kV, it is also sensitive to the variation in the reactive flow coming from the LTS that connects it to the system; it presents a small voltage variation, since it is connected to the PV plant that controls the reactive.

4.1.5. Scenario 5—Contingency Analysis with PV Generation under Conditions of 100% PV Generation Increment

For scenario 5, the contingency was analyzed in the section of the studied system, where the steady-state contribution of the PV system was simulated within the electrical generation limits defined for a condition of 100% of the PV generation increase predicted for the PV complex, i.e., the PV contribution was considerably increased in the system section. The system model was the same as that inserted in the simulation of previous cases, but with the necessary adjustments corresponding to scenario 5. Thus, PV generation started to provide 270 MW of active power. The insertion limit of reactive power (MVAr) of the PV plant was also adjusted to a value of 55 MVAr. The change in the reactive power limit was performed to keep the power factor of the PV plant in the range of 0.95 inductive or capacitive, as defined in submodule 3.2 of the Grid Procedures. As in the first case, the shutdown of shunt reactor of 5408 (MILAGR-CE500), which is connected to the 500 kV miracle bus, and static compensator 5410 (MILAGRCER230) connected to the 230 kV miracle bus was also considered as a contingency situation.

Then, changes in the voltage levels of the same buses defined for scenario 4 were analyzed, through the new PV configuration, for situations with and without contingency. The steady-state variations of the voltages in the selected buses were determined under non-contingency conditions (with regulation equipment connected to the system) and contingency conditions (loss of regulation equipment).

Initially, when scenario 5 and scenario 3 are compared, still under normal operating conditions, it is possible to observe a decrease in the voltages of the buses closer to the PV generation. This happens because, as the generation from the PV plant (related to scenario 2) considerably increased, it generated a reverse flow of active energy through the lines in the opposite direction of the loads, resulting in a constant increase in the flow of reactive power (consumed by the LTS series reactance) and decrease in bus voltage magnitudes. Other buses closer to the traditional generation (distant from the PV generation and close to the traditional generation) had a slight increase in voltage, even with a decrease in active power (supplied by the PV generation), since they had effective control of the reactive

power flow accomplished by synchronous generators. Another highlight in the initial comparison would be bus 5959 (RIOALT-PB034), whose voltage level is 34 kV and which is where the PV plant is connected. We can observe that there was a more relevant initial voltage drop, due to the fact that this bus is connected to the system through LTS with lower nominal voltages; therefore, they have low susceptance (shunt parameter), so they are very sensitive to the active power flow, which in this case was generated by increasing the PV contribution. However, the PV system manages to attenuate this voltage drop effect, through the reactive control in the bus.

In relation to the comparative analysis of the voltage levels in the bars in the normal condition, in the condition of maximum penetration (scenario 3) and in the contingency condition defined for scenario 5, despite having an increase in the voltage levels of bars 5621 (COREMA- PB230) and 5623 (COREMA-PB069), rising from 0.991 pu to 1.002 pu and from 1.008 pu to 1.019 pu, respectively, there was a smaller variation than evidenced with little PV generation in the contingency situation (scenario 4). This small variation ensured that the voltage profile was kept away from the upper limits of 1.05 pu. Figure 12 brings a comparison of voltage growth in all buses verified in this study, with emphasis on the two COREMAS buses, in which the PV generation is connected.

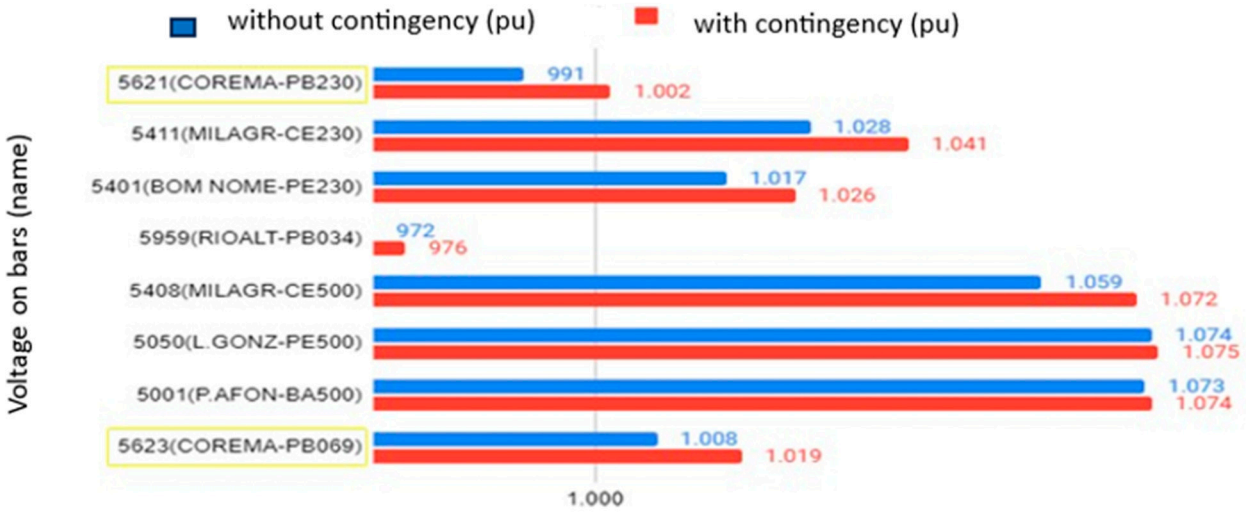


Figure 12. Quantitative representation of the voltage levels per bus before and after the contingency under the conditions foreseen for the second case (100% increment). Source: the authors.

Analyzing the graph in Figure 12 as well as scenario 4, it is possible to infer that all buses had an increase in voltage level when the system lost the two control devices. At points furthest from the control elements and close to traditional (hydroelectric) generation, such as buses 5050 (L.GONZ-PE500) and 5001 (P.AFON-BA500), once again, there was virtually no voltage variation. At the points closest to the reactive control elements that were turned off and far from the PV plant, such as bus 5408 (MILAGR-CE500), a significant voltage variation was observed, going from 1059 pu to 1072 pu; however, there was a variation smaller than what occurred in scenario 4 (with little PV generation). All buses closer to the PV plant had variations in minor stress levels compared to the first case. This smaller variation was the result of the decrease in reactive from PV generation (reactive control), causing the flow of reactive in nearby buses to increase again and offset the decrease in reactive, due to the removal of reactive absorption equipment.

5. Conclusions

The study carried out in this article made it possible to analyze the impacts of the gradual and increasing insertion of centralized photovoltaic systems into a high-voltage electrical transmission network. Using real data from the northern section of the Eletrobrás-Chesf transmission system, focusing on the Coremas-PB substation, simulations were

carried out on the transmission system, based on various scenarios, to identify and observe voltage levels in bars close to the insertion PV, separated by long lines and close to the traditional generators of the section of the network with a significant increase in solar photovoltaic generation.

The comparative analysis was performed considering different levels of photovoltaic insertion in the transmission system. Three scenarios were defined: the first representing the current operating condition with 70 MW of photovoltaic generation; the second with the insertion of 50% of the nominal power of the photovoltaic plant (170 MW); the third with the complete insertion of the foreseen capacity (270 MW). Two contingency scenarios were also analyzed: scenario 4, with the current PV insertion (70 MW) and the shutdown of two pieces of equipment, and scenario 5, with the total PV insertion expected to come into operation and the loss of the same equipment simulated in scenario 4.

Under normal operating conditions, it was evident that with the increase in the PV insertion in the simulated conditions, there was a more significant drop in bus voltages close to the photovoltaic complex. Regarding the decrease in voltage profiles, there was a satisfactory approximation of 1 pu per module, in accordance with the electrical transmission quality criteria.

In this study of the contingency situation, in which the equipment that absorbs system reactants was turned off, scenario 4, which compared the bus voltage levels in the contingency and normal operating situations, showed a significant difference in the voltage modules (increase voltage) in the bars close to the photovoltaic generators but maintained levels within the maximum permissible limits. In scenario 5, the variations in voltage levels were considerably smaller than in scenario 4. This difference was the result of the effective contribution of the increase in PV generation, reducing the final voltages of the buses after the contingencies. No scenario showed significant differences evident in bars closer to conventional generation. Therefore, it was evident that, in the contingency condition being studied, the increase in photovoltaic insertion contributed to the stability of the voltage profiles in the bars.

These results are of great relevance for the planning and operation of an electrical system, as they provide valuable information on the impacts of inserting photovoltaic generation into a high-voltage transmission network. Studies on the Brazilian transmission network with PV insertion still need to be expanded, as they provide technical security for future expansions of this type of generation in the transmission system. It was also possible to infer from the results that the contribution of PV generation reduced the number of maneuvers and the use of regulation equipment, such as transformer switches, reactors, capacitor banks, and synchronous and static compensators, within a horizon of operations.

Based on these analyses, it is possible to adequately plan for the insertion of large levels of PV generation into the transmission network to guarantee the stability, quality, and reliability of the electrical energy supply, considering both normal operation and contingency situations. An analysis of the spatial distribution of PV insertion in the system would also be relevant.

Author Contributions: Conceptualization, F.X.L., G.F.d.N., I.C.T. and C.T. All authors have read and agreed to the published version of the manuscript.

Funding: We gratefully thank to UFPE—Universidade Federal de Pernambuco, DEN—Departamento de Energia Nuclear, and Conselho Nacional de Pesquisa (CNPq) Grant No. 310213/2021-5, for supporting the material means and the scientific environment for the execution of this research. This research was funded by Fundação Coordenação de Aperfeiçoamento de Pessoal de Nível Superior (Capes) grant number 88887.801241/2023-00, for supporting the material means and the scientific environment for the execution of this research.

Conflicts of Interest: The authors declare no conflict of interest.

References

1. Remund, J.; Ramirez, L.; Wilbert, S.; Blanc, P.; Lorenz, E.; Köhler, C.; Paristech, M. Solar Resource for High Penetration and Large-Scale Applications. In Proceedings of the 33rd European Photovoltaic Solar Energy Conference and Exhibition PVSEC, Amsterdam, The Netherlands, 25–29 September 2017; p. 40.
2. IEA PVPS Reporting Countries, Becquerel Institute (BE). For the Non-IEA PVPS Countries: Izumi Kaizuka (RTS; Corporation), Arnulf Jäger-WALDAU (EU-JRC), Jose Donoso (UNEF). Snapshot of Global PV Markets 2023. [S.l: s.n.]. 2023. Available online: https://iea-pvps.org/wp-content/uploads/2023/04/IEA_PVPS_Snapshot_2023.pdf (accessed on 13 February 2023).
3. ANEEL—Agência Nacional de Energia Elétrica. 2023. Available online: https://www.gov.br/aneel/pt-br/assuntos/noticias/2023/primeiro-semestre-de-2023-tem-crescimento-de-5-1-gw-na-matriz-eletrica-brasileira (accessed on 13 June 2023).
4. ANEEL. *Atlas de Energia Elétrica do Brasil*, 3rd ed.; Agência Nacional de Energia Elétrica: Brasília, Brazil, 2008. Available online: https://www.fisica.net/energia/atlas_de_energia_eletrica_do_brasul_3a-ed.pdf (accessed on 13 December 2021).
5. Pereira, E.B.; Martins, F.R.; Gonçalves, A.R.; Costa, R.S.; Lima, F.L.; Rüther, R.; Abreu, S.L.; Tiepolo, G.M.; Pereira, S.V.; Souza, J.G. *Atlas Brasileiro de Energiaslar*, 2nd ed.; Instituto Nacional de Pesquisas Espaciais (INPE): São José, Brazil, 2017.
6. Pinho, J.T.; Galdino, M.A. Manual de Engenharia para Sistemas Fotovoltaicos. Rio de Janeiro: CEPEL/CRESESB. 2014. Available online: http://www.cresesb.cepel.br/publicacoes/download/Manual_de_Engenharia_FV_2014.pdf (accessed on 20 December 2021).
7. Ruschel, C.S.; Santucci, A.; Oliveira, B. Evolução das Características Técnicas dos Projetos Fotovoltaicos nos Leilões de Energia do Mercado Regulado. 2014. Available online: https://anaiscbens.emnuvens.com.br/cbens/article/download/981/981 (accessed on 13 December 2022).
8. Villalva, M.G. *Energia Solar Fotovoltaica: Conceitos e Aplicações*, 2nd ed.; Saraiva: São Paulo, Brazil, 2015.
9. EPE. Plano Nacional de energia 2050. Ministério de Minas e Energia. Empresa de Pesquisa Energética. Energética. Brasília: MME/EPE. 2022. Available online: https://www.gov.br/mme/pt-br/assuntos/secretarias/sntep/publicacoes/plano-nacional-de-energia/plano-nacional-de-energia-2050 (accessed on 22 February 2022).
10. Stevenson, W.D., Jr. *Elementos de Análise de Sistemas de Potência*; McGraw-Hill Education do Brasil: São Paulo, Brazil, 1978.
11. EPE. Plano Decenal de Expansão de Energia 2029. Ministério de Minas e Energia. Empresa de Pesquisa Energética. Brasília: MME/EPE. 2020. Available online: https://www.epe.gov.br/sites-pt/publicacoes-dados-abertos/publicacoes/Documents/PDE%202029.pdf (accessed on 1 January 2021).
12. Kumar, D.S.; Sharma, A.; Srinivasan, D.; Reindl, T. Stability implications of bulk power net works with large scale PVs. *Energy* **2019**, *187*, 115927. [CrossRef]
13. Denholm, P.; O'Connell, M.; Brinkman, G.; Jorgenson, J. *Overgeneration from Solar Energy in California: A Field Guide to the Duck Chart*; Technical Report, November, 2015; Office of Energy Efficiency & Renewable Energy: Golden, CO, USA, 2015.
14. Matarucco, R.R. Método da Continuação Aplicado na Análise de Contingência de Linhas de Transmissão. Ph.D. Thesis, Universidade Estadual Paulista, São Paulo, Brazil, 2010.
15. ONS. Balanço de Energia. Available online: https://www.ons.org.br/paginas/energia-agora/balanco-de-energia (accessed on 22 December 2022).
16. Zhang, Y.; Mensah-bonsu, C.; Walke, P.; Arora, S.; Pierce, J. Transient over-voltages in high voltage grid-connected PV solar interconnection. In Proceedings of the IEEE PES General Meeting, Minneapolis, MN, USA, 25–29 July 2010; p. 1e6.
17. Martins, T.U. *Estudos Elétricos para Conexão à Rede Básica de Uma Central Geradora Solar Fotovoltaica Utilizando a Ferramenta Computacional Anarede*; Monografia (Graduação em Engenharia Elétrica); Universidade Federal do Ceará: Fortaleza, Brazil, 2019; p. 19.
18. Luque, A.; Hegedus, S. (Eds.) PV Systems. In *Handbook of Photovoltaic Science and Engineering*, 2nd ed.; Wiley: Hoboken, NJ, USA, 2012.
19. Torres, I.C.; Chigueru, T.; Negreiros, G.F. Impacto da Instalação Massiva de Sistemas FV Distríbuidos no Nível de Tensão da Rede de Distribuição Elétrica de Baixa Tensão. VIII Congresso Brasileiro de Energia Solar. Fortaleza, Ceará. Available online: http://www.abens.org.br/CBENS2020/home/ (accessed on 20 January 2022).
20. Resende, J.W. *Introdução a Compensação Reativa: Apostila da Disciplina Carga Elétricas não Convencionais na Rede Elétrica: Uberlândia*; Universidade Federal de Uberlândia: Uberlândia, Brazil, 2020.
21. Paludo, J.A. Avaliação dos Impactos de Elevados Níveis de Penetração da Geração Fotovoltaica no Desempenho de Sistemas de Distribuição de Energia Elétrica em Regime Permanente. Master's Thesis, Escola de Engenharia de São Carlos da Universidade de São Paulo, São Carlos, Brazil, 2014.
22. ANEEL—Agência Nacional de Energia Elétrica. Procedimentos de Rede, Módulo 2—Critérios e Requisitos, Submódulo 2.3 -Premissas, Critérios e Metodologia para estudos elétricos, Revisão 12. Resolução normativa nº 903/2020. 2021; pp. 1–35.
23. CHESF. Subestação Coremas. Dados fornecidos pela empresa. 2021. Available online: https://www.chesf.com.br/Pages/default.aspx (accessed on 22 December 2022).
24. Family Search. Coremas, Paraíba: Genealogia. Available online: https://www.familysearch.org/wiki/pt/Coremas,_Para%C3%ADba_-_Genealogia (accessed on 13 December 2021).
25. Google Earth. Coremas. 2020. Available online: https://earth.google.com/web (accessed on 13 December 2021).
26. ONS. Procedimentos de Rede. Operador Nacional do Sistema. 2020. Available online: https://www.ons.org.br/paginas/sobre-o-ons/procedimentos-de-rede/vigentes (accessed on 22 December 2021).

27. Oliveira, E.H.G.D. Análise Estática de Contingências do Sistema de Transmissão de 230 kV do Acre / Rondônia. 2019. Available online: https://bdm.unb.br/bitstream/10483/24373/1/2019_EduardoHenriqueGomesDeOliveira_tcc.pdf (accessed on 18 December 2020).
28. Monticelli, A.J. *Fluxo de Carga em Redes de Energiaelétrica*; Edgard Blücher: São Paulo, Brazil, 1983.

Disclaimer/Publisher's Note: The statements, opinions and data contained in all publications are solely those of the individual author(s) and contributor(s) and not of MDPI and/or the editor(s). MDPI and/or the editor(s) disclaim responsibility for any injury to people or property resulting from any ideas, methods, instructions or products referred to in the content.